

Femtosecond XUV-IR dynamics of the methyl iodide cation

Geert Reitsma^{1,†}, *Marta L. Murillo-Sánchez*², *Rebeca de Nalda*³, *Mariu E. Corrales*²,
Sonia Marggi Poullain^{2,4}, *Jesús González-Vázquez*^{4,5}, *Marc J.J. Vrakking*¹, *Luis Bañares*²
and *Oleg Kornilov*¹

¹Max Born Institute for Nonlinear Optics and Short Pulse Spectroscopy, Max-Born-Strasse 2A, 12489 Berlin, Germany.

²Departamento de Química Física (Unidad Asociada I+D+i al CSIC), Facultad de Ciencias Químicas, Universidad Complutense de Madrid, 28040 Madrid, Spain.

³CSIC, Instituto Química Física Rocasolano, C/Serrano 119, E-28006 Madrid, Spain.

⁴Departamento de Química, Facultad de Ciencias, Universidad Autónoma de Madrid, Módulo 13, 28049 Madrid, Spain.

⁵Institute for Advanced Research in Chemical Sciences (IAdChem), Facultad de Ciencias, Universidad Autónoma de Madrid, 28049, Spain.

Abstract. Wavelength-selected laser pulses obtained from high harmonic generation are an excellent tool to study the dynamics of cations state-by-state. We demonstrate this by pump-probe experiments on CH₃I molecules and unravel both resonant and non-resonant dynamics.

1 Introduction

Ultrashort extreme ultraviolet (XUV) pulses obtained from high harmonic generation (HHG) allow for studies of dynamics in molecular cations. Typical experiments using HHG have excellent time-resolution and can access processes such as charge migration [1], evolution of vibrational wavepackets [2], and fast decays through conical intersections [3]. However, in experiments using the full bandwidth of HHG sources, signals from different states are mixed, which makes interpretation often difficult. Here, we employ a time-delay-compensating XUV monochromator [4] which defines the photon energy and allows to study state-by-state and also to distinguish processes in cations from those in highly excited neutrals, because the former are present with all harmonics of sufficient energy and the latter are resonant and thus only present with a selected harmonic. The monochromator delivers selected harmonics, obtained from the output of an HHG-source, with a spectral bandwidth of 300 meV and a time duration of 20-25 fs. To perform pump-probe experiments, the wavelength-selected XUV beam is recombined with 25 fs IR pulses. In the present contribution we investigate cationic states of the CH₃I molecule. The dissociation of the CH₃I⁺ cation along the C-I axis is mainly governed by a geometry change in the methyl part from pyramid to planar and the spin-orbit splitting in the iodine atoms. The latter

† Corresponding author: reitsma@mbi-berlin.de

induces avoided crossings in the manifold of potential energy surfaces which make CH_3I^+ dissociation particularly interesting.

2 Results and Discussion

In the experiments, we used three harmonics: 7, 9, and 11 from the 800nm fundamental driving pulse. With $E_{\text{ph}} = 10.9$ eV (harmonic 7), only the spin-orbit split ground state ($X^2E_{3/2,1/2}$) can be populated. With the next high harmonic $E_{\text{ph}} = 14.0$ eV (harmonic 9), the weakly bound first excited state (A^2A_1) is populated as well, while harmonic 11 ($E_{\text{ph}} = 17.1$ eV) also reaches the repulsive B^2E state. Note that at these photon energies also Rydberg series converging to the respective excited cations can be resonantly excited, leading to fluorescence, auto-ionization, or neutral dissociation processes. For each harmonic we recorded velocity map images for both the CH_3I^+ and I^+ fragment, demonstrating both dynamics in the cation as well as dynamics of resonant neutral states.

With $E_{\text{ph}} = 10.9$ eV photons, no decay dynamics in the cation are expected upon ionization to the $X^2E_{3/2,1/2}$ ground state as the states are bound and their vibrational activity is negligible [5]. However, in the experiment we observe an enhancement of the signal at temporal overlap followed by a decay. This behavior cannot be explained by cation dynamics, and therefore must come from neutral dissociation signal upon resonant absorption. This is supported by the fact that it is not observed for higher harmonics. Previous photo-absorption studies indeed have identified Rydberg series converging to the A^2A_1 and B^2E potential energy surfaces [6]. Calculations are currently in progress to establish with certainty which of these states are responsible for the observed behavior and to explain the observed 90 fs timescale.

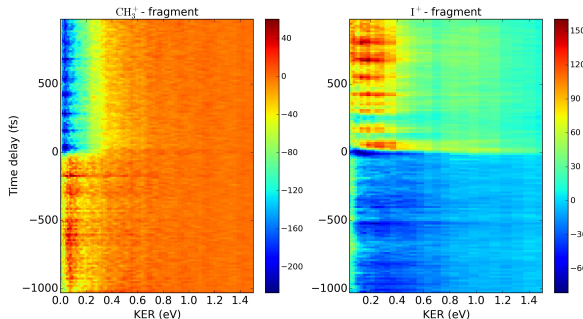


Fig 1. Time-dependent kinetic energy release maps of the CH_3^+ (a) and I^+ (b) obtained with a 17.2 eV XUV pump pulse and an IR probe pulse. A positive delay means that the IR pulse comes after the XUV pulse.

For photon energies of 14.0 and 17.1 eV we obtain very comparable data, both different from 10.9 eV. Figure 1 displays maps of the total kinetic energy release (KER) as a function of time delay for dissociation into $\text{I} + \text{CH}_3^+$ and $\text{CH}_3 + \text{I}^+$, obtained for the $E_{\text{ph}} = 17.1$ eV pump and IR probe scheme. When IR comes after XUV, the yield of CH_3^+ fragments decreases while the yield of I^+ fragments is enhanced. On top of this long lived contribution, clear oscillatory signals are observed in both ionic fragment yields. The period of this oscillation is 127 ± 3 fs and the oscillations in the CH_3^+ and I^+ yield are in opposite phase with respect to each other.

The observed frequency closely corresponds to the frequency of the C-I stretching mode in the A^2A_1 state [7]. Therefore we interpret the observation as follows. The A^2A_1 state is populated at the inner turning point of the potential well, launching a wavepacket composed of several vibrational states. In the XUV-only experiment the most common

dissociation pathway would be a non-adiabatic coupling to hot vibrational bands in the spin-orbit split ground state of the cation $X^2E_{3/2,1/2}$. The molecule then statistically dissociates producing CH_3^+ . The latter mechanism is consistent with the discrepancy between lifetime of the A^2A_1 state (10^{-10} s) and the dissociation rate constant 10^{-7} s) [7,8]. The low total KER for the dissociation into $\text{I} + \text{CH}_3^+$ is also consistent with this scenario.

The IR pulse couples the A^2A_1 state population to a repulsive potential energy surface leading to dissociation into $\text{CH}_3 + \text{I}^+$. As this state serves as a common final state for the coherently populated vibrational levels in the A^2A_1 state, these pathways interfere with a beating frequency equivalent to the energetic separation between those states. The fact that dissociation into $\text{CH}_3 + \text{I}^+$ occurs with a nonzero KER corresponds to energy separation. Inherently, the $\text{I} + \text{CH}_3^+$ dissociation channel should exhibit the same oscillation, but with opposite sign.

To complete the picture, it is necessary to know the exact probing mechanism induced by the IR. The potential energy surfaces of reference [9] can qualitatively describe the probing step. Further calculations are underway to obtain further insight into the role of the IR field on the coupling to dissociative states.

3 Conclusion

We used wavelength-selected XUV pulses to study the lowest states of the CH_3I^+ cation. We observed dynamics upon resonant absorption by members of Rydberg series converging to these states as well as a vibrational wavepacket that can be used to steer the dissociation to either the $\text{I} + \text{CH}_3^+$ or the $\text{CH}_3 + \text{I}^+$ channel depending on the phase of the wavepacket at the arrival time of the probe pulse. We aim to quantify this control process with the help of potential energy surface calculations on which a wavepacket will be propagated with the IR field implemented.

References

- [1] F. Calegari, D. Ayuso, A. Trabattoni, L. Belshaw, S. De Camillis, S. Anumula, F. Frassetto, L. Poletto, A. Palacios, P. Declava, J. B. Greenwood, F. Martin, and M. Nisoli, *Science* **346**, 336-339 (2014).
- [2] F. Kelkensberg, C. Lefebvre, W. Siu, O. Ghafur, T. T. Nguyen-Dang, O. Atabek, A. Keller, V. Serov, P. Johnsson, M. Swoboda, T. Remetter, A. L'Huillier, S. Zherebtsov, G. Sansone, E. Benedetti, F. Ferrari, M. Nisoli, F. Lepine, M. F. Kling, and M. J. J. Vrakking, *Phys. Rev. Lett.* **103**, 123005 (2009).
- [3] M. C. E. Galbraith, S. Scheit, N. V. Golubev, G. Reitsma, N. Zhavoronkov, V. Despre, F. Lepine, A. I. Kuleff, M. J. J. Vrakking, O. Kornilov, H. Koepfel, and J. Mikosch, *Nature Communications*. **8**, 1018 (2017).
- [4] M. Eckstein, C.-H. Yang, M. Kubin, F. Frassetto, L. Poletto, H.-H. Ritze, M. J. J. Vrakking, and O. Kornilov, *J. Phys. Chem. Lett.* **6**, 419-425 (2015).
- [5] L. Karlsson, R. Jadrny, L. Mattsson, F. Chau, and K. Siegbahn, *Phys. Scr.* **16**, 225-234 (1977).
- [6] R. Loch, B. Leyh, H. W. Jochims, and H. Baumgaertel, *Chem. Phys.* **365**, 109-128 (2009).
- [7] S. Goss, D. Mcgilvery, J. Morrison, and D. Smith, *J. Chem. Phys.* **75**, 1820-1828 (1981).
- [8] D. Mintz and T. Baer, *J. Chem. Phys.* **65**, 2407-2415 (1976).
- [9] S. Marggi Poullain, D. V. Chicharro, J. Gonzalez-Vazquez, L. Rubio-Lago, and L. Banares, *Phys. Chem. Chem. Phys.* **19**, 7886-7896 (2017).